


Magnonic Analog of Black- and White-Hole Horizons in Superfluid $^3\text{He-B}$

M. Človečko, E. Gažo, M. Kupka, and P. Skyba*

Institute of Experimental Physics, SAS and P. J. Šafárik University Košice, Watsonova 47, 04001 Košice, Slovakia
 (Received 18 April 2019; published 16 October 2019)

We report on the theoretical model and experimental results of the experiment made in a limit of absolute zero temperature ($\sim 600 \mu\text{K}$) studying the spin wave analog of black- and white-hole horizons using spin (magnonic) superfluidity in superfluid $^3\text{He-B}$. As an experimental tool simulating the properties of the black- and white-hole horizons, we used the spin-precession waves propagating on the background of the spin supercurrents between two Bose-Einstein condensates of magnons in the form of homogeneously precessing domains. We provide experimental evidence of the white hole formation for spin precession waves in this system, together with the observation of an amplification effect. Moreover, the estimated temperature of the spontaneous Hawking radiation in this system is about 4 orders of magnitude lower than the system's background temperature which makes it a promising tool for studying the effect of spontaneous Hawking radiation.

DOI: 10.1103/PhysRevLett.123.161302

Recently, it has been shown that Hawking radiation should be related not only to physics of the astronomical black holes [1], but should also be viewed as a general phenomenon of a dynamic nature of various physical systems having capability, at certain conditions, to create and form a boundary—an event horizon [2]. According to theory, a fundamental dynamical property of any event horizon analog is a spontaneous emission of thermal Hawking radiation, the temperature of which depends on a velocity gradient at the horizon [3,4]

$$T = \frac{\hbar}{2\pi k_B} \frac{\partial v^r}{\partial r} \sim 10^{-12} \frac{\partial v^r}{\partial r}. \quad (1)$$

Among a set of physical systems used to model black- and white-hole horizons, the sound waves in trans-sonic fluid flow [3,5], the surface waves on flowing fluid [6–10], hydraulic jumps in flowing liquids [11–13], one dimensional polariton fluid [14], type-II Weyl fermions in topological Weyl semimetals [15] and light in optical fibre [16], and other dispersive media [17] can be included. It turns out, however, that the temperature of the spontaneous Hawking radiation is typically several orders of magnitude lower than the background temperature of the physical systems used as an experimental tool in studying this phenomenon. Perhaps the solution to this problem is to find another suitable condensed matter system which can model the event horizon, but with a background temperature approaching absolute zero temperature [18–22].

In this Letter, we present as a theoretical model, and so, experimental results of the first experiment made in a limit of absolute zero temperature ($\sim 600 \mu\text{K}$) studying the black- and white-hole horizon analog using a physical quantum system based on the spin (magnonic) superfluidity

in superfluid $^3\text{He-B}$. The concept of the experiment is quite simple [23]. The experimental cell with superfluid $^3\text{He-B}$ consists of two cylinders mutually connected by a channel (see Fig. 1). The cell is placed in a steady magnetic field B_0 and magnetic field gradient ∇B , both oriented along z axis. Using a cw NMR technique, we created a Bose-Einstein condensate of magnons in the form of the homogeneously precessing domain (HPD) in both cylinders

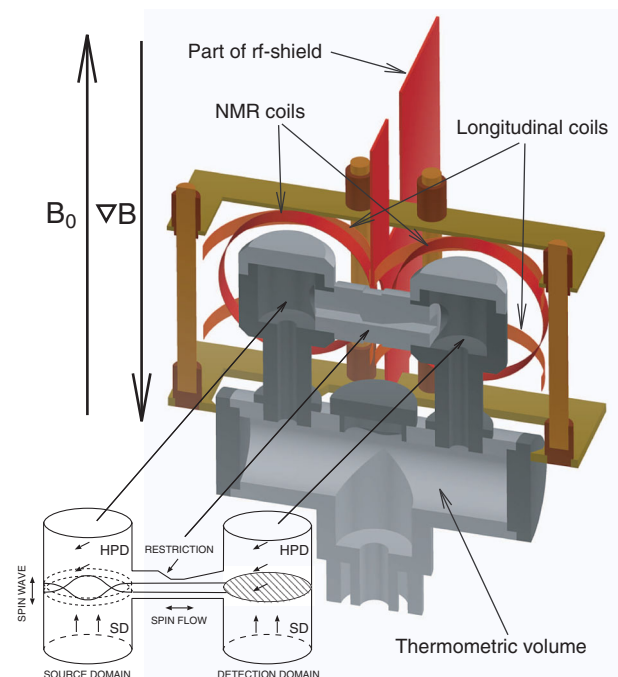


FIG. 1. Schematic 3D cross section of the experimental cell and concept of the experiment. Channel dimensions: the width is 3 mm, the height is 0.4 mm, and the channel length is 2 mm.

[24–26]. The HPD is a dynamical spin structure formed in a part of the cell placed in a lower magnetic field which, with the aid of the dipole-dipole interaction, coherently precesses around a steady magnetic field at the angular frequency ω_{rf} . Within the rest of the cell, the spins are codirectional with the steady magnetic field and do not precess thus forming a stationary domain (SD). These two spin domains are separated by a planar domain wall, the position of which is determined by the Larmor resonance condition $\omega_{\text{rf}} = \gamma(B_0 + \nabla B z)$, where γ is the gyromagnetic ratio of the ^3He nuclei.

To model black- and white-hole horizons in superfluid $^3\text{He-B}$, we used two fundamental physical properties of the HPD: the spin superfluidity and the presence of the HPD's collective oscillation modes in the form of the spin precession waves [27–34]. The spin superfluidity allows us to create and manipulate the spin flow, i.e., the spin supercurrents flowing between precessing domains as a consequence of the phase difference $\Delta\alpha_{\text{rf}}$ between the phases of spin precession in individual domains [35]. The spin precession waves serve as a probe testing formation and the presence of black- and white-hole horizons inside the channel: the channel has a restriction allowing us to reach the different regimes of the velocity of the spin supercurrent flow with respect to the group velocity of the traveling spin-precession waves. This is similar to the experiment suggested by Schützhold and Unruh [6] and later performed by Rousseaux *et al.* [7–9] and Weinfurter *et al.* [10]. However, to compare with the above mentioned classical water wave experiments, the quantum coherent system based on the spin (or magnonic) superfluidity in $^3\text{He-B}$ exhibits a much broader portfolio of the fundamental physical properties allowing us to investigate the quantum effects on the horizon, on one side, and also offers higher experimental variability and controlling on the second side (see [36] for details).

In order to develop a mathematical model, we initially considered a simplified problem—a volume of $^3\text{He-B}$ placed into a large steady magnetic field B_0 with gradient field ∇B applied in the z direction and a small magnetic rf field B_{rf} , which rotates in the “horizontal” x - y plane at the angular frequency ω_{rf} , with the phase of rotation varying linearly with x . Cartesian components of the resultant magnetic field are $B_x = -B_{\text{rf}} \cos(\omega_{\text{rf}}t + \nabla\alpha_{\text{rf}}x)$, $B_y = B_{\text{rf}} \sin(\omega_{\text{rf}}t + \nabla\alpha_{\text{rf}}x)$ and $B_z = -B_0 + \nabla B z$. This model problem is treated theoretically by adapting the method we presented elsewhere [34].

The steady-state response is a layer of magnetization precessing with the frequency and local phase of the rf field lying over a layer of stationary magnetization. The domain with precessing spins (magnetization) may oscillate about its steady state. The principal variable describing small oscillations is the perturbation $a(t, x, y, z)$ to the phase of spin precession. In the long wavelength approximation and for a thin domain of precessing spins, the perturbation

propagating along the domain wall is found to be governed by the equation

$$\left(\frac{\partial}{\partial t} - \frac{\partial}{\partial x} u\right) \left(\frac{\partial}{\partial t} - u \frac{\partial}{\partial x}\right) a_{\text{DW}} - \frac{\partial}{\partial x} \left(c^2 \frac{\partial a_{\text{DW}}}{\partial x}\right) - \frac{\partial}{\partial y} \left(c^2 \frac{\partial a_{\text{DW}}}{\partial y}\right) + \sqrt{\frac{3}{5}} \gamma^2 \nabla B B_{\text{rf}} L a_{\text{DW}} = 0. \quad (2)$$

Here, $a_{\text{DW}}(t, x, y) = a(t, x, y, z_{\text{DW}})$, where z_{DW} denotes the z coordinate of the domain wall position, and L is the thickness of the precessing domain. Two terms u and c represent the spin flow and the group wave velocities, respectively, and they can be expressed as

$$u = \frac{(5c_L^2 - c_T^2) \nabla\alpha_{\text{rf}}}{2\omega_{\text{rf}}}, \quad c^2 = \frac{(5c_L^2 + 3c_T^2) \gamma \nabla B L}{4\omega_{\text{rf}}}, \quad (3)$$

where c_L and c_T denote the longitudinal and transverse spin wave velocities with respect to the field orientation, respectively. We shall assume that $\nabla\alpha_{\text{rf}}$ is localized on the length of the sharpest restriction in the channel of the order $dl = 0.5$ mm, therefore, $\nabla\alpha_{\text{rf}} \sim \Delta\alpha_{\text{rf}}/dl$.

The long spin-precession waves traveling along the surface of a thin layer of precessing and flowing spins are governed by the same equation as a scalar field in a $(2+1)$ -dimensional curved space-time. Thus, these waves experience the background as an effective space-time with the effective metric

$$ds^2 = c^2[-c^2 dt^2 + (dx + u dt)^2 + dy^2]. \quad (4)$$

As is implied by this equation, an “event horizon” for the long spin-precession waves is formed where and when $u^2 = c^2$. For the sake of completeness, the exact dependence of the angular frequency ω of any spin-precession wave on components k_x and k_y of its wave vector is

$$(\omega + uk_x)^2 = \frac{\gamma \nabla B}{2\omega_{\text{rf}}} c_1^2 \kappa \tanh(\kappa L), \quad (5)$$

where $c_1^2 = (5c_T^2 - c_L^2)$ and κ is defined as

$$\kappa^2 = \frac{3}{2c_1^2} \left[\frac{4}{\sqrt{15}} \omega_{\text{rf}} \gamma B_{\text{rf}} + \frac{1}{3} (5c_L^2 + 3c_T^2) (k_x^2 + k_y^2) \right]. \quad (6)$$

It is important to note that the applied rf field explicitly determines the “vacuum,” that is to say, it prescribes the angular frequency and the variation of the phase for the precessing magnetization (spins) representing a steady state of the system considered. But Eq. (2), for small oscillations superposed on the steady state, is determined primarily by the properties of that state, no matter how the steady state was created (except for the “mass” term that is determined by the external field explicitly). So, Eq. (2) is capable of describing the perturbations of the steady state in the

absence of rf field if the precession of background magnetization has maintained its given angular frequency and phase. Although derived for a background represented by a uniform magnetization flow parallel to the flat top of the cell, the above presented relations can be used for qualitative analysis and quantitative estimation of the situation where $\nabla\alpha_{\text{rf}}$ and L slightly vary on spatial scales larger than L .

As mentioned above, we performed the experiment in the cell shown in Fig. 1. The cell was attached to Košice's diffusion nuclear stage [39], filled with ^3He at three bars and using the adiabatic demagnetization cooled down to a temperature of $\sim 0.5 T_c$. The temperature of the ^3He was measured using a powder Pt NMR thermometer immersed in the liquid and calibrated against the ^3He superfluid transition temperature T_c . The HPDs were simultaneously and independently excited in both cells using a cw NMR method at angular frequency $\omega_{\text{rf}} = 2\pi \times 462 \times 10^3$ rad/sec. To achieve this, we used two rf generators working in phase-locked mode and with zero phase difference $\Delta\alpha_{\text{rf}}$ between excitation signals. The induced voltage signals from NMR coils were amplified by preamplifiers and measured by two rf lock-in amplifiers, each controlled by its own generator. In order to reduce the mutual crosstalk between the rf coils, each rf coil was covered by a shield made of copper foil. The longitudinal coils provided an additional alternating magnetic field used for the spin-precession wave generation [32].

Once two HPDs were generated, the position of the domain wall was adjusted into the channel [40]. This step is easy to accomplish by means of the homogeneous field B_0 (with the aid of small longitudinal oscillations), as the position of the domain wall follows the plane where the Larmor resonance condition is satisfied. Specifically, the precision of the domain wall adjustment is given by $\Delta B_0/\nabla B$, where $\Delta B_0 = 0.76 \mu\text{T}$ is the field step controlled by the current source and for $\nabla B = 15$ mT/m giving a spatial precision of $\sim 50 \mu\text{m}$ [41]. For comparison, the domain wall thickness $[\lambda_F = c_L^{2/3}/(\gamma\nabla B\omega_{\text{rf}})^{1/3}]$ for the above parameters is ~ 0.34 mm. As the height of the channel is 0.4 mm, an estimated length of the precessing layer L in the channel is $L \sim 150 \mu\text{m} \pm 50 \mu\text{m}$. The spin flow between HPDs can be established in both directions depending on the sign of the phase difference $\Delta\alpha_{\text{rf}}$, while the spin flow velocity u depended on the magnitude of $\Delta\alpha_{\text{rf}}$. The details of the experiment are provided in [36].

The spin-precession waves in the source domain were generated by eight sinusoidal pulses at an appropriately low frequency using a separate generator. The low frequency response from the source and detection of the HPD for a particular value of $\Delta\alpha_{\text{rf}}$ was extracted from rf signal by a technique based on the application of a rf detector and a low-frequency filter. The low frequency signals were stored by a digital oscilloscope for the data analysis. The examples of the signals representing the excited spin-precession wave

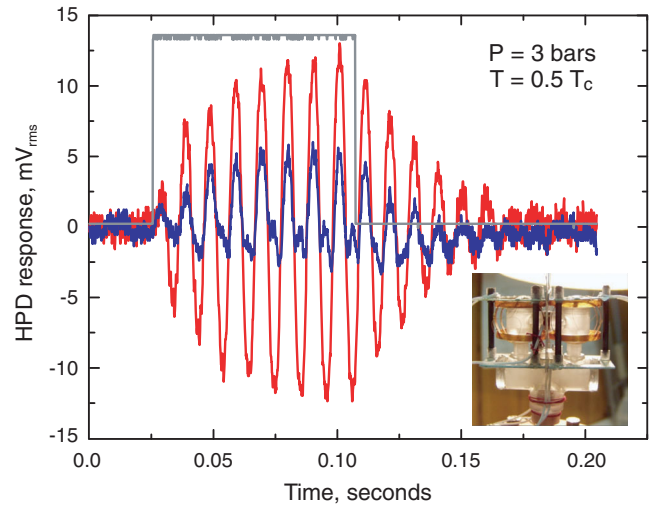


FIG. 2. Voltage signals corresponding to spin-precession waves: the source domain (red), the detection domain (blue). The rectangular signal shows the time window when eight sinusoidal excitation pulses were applied in order to excite the spin-precession waves. Inset: the picture of the experimental cell on the bench before rf-shield installation.

in the source domain and incoming wave in the detection domain are shown in Fig. 2. When the pulse is finished, there are clear free decay signals of the spin-precession waves from both domains, and these parts of the signals were analyzed by the methods of the spectral analysis as a function of the phase difference $\Delta\alpha_{\text{rf}}$, i.e., as a function of the spin flow velocity u .

Figure 3 shows the power spectral density (PSD) of the free decay signals for the source (upper) and detection (lower) domains as a function of the phase difference $\Delta\alpha_{\text{rf}}$. There are a few remarkable features presented there. Firstly, there are relatively strong PSD signals in the source domain with the exception of a deep minimum at the region of $\Delta\alpha_{\text{rf}}$ corresponding to $\sim 10^\circ$. Second, the weaker PSD signals are observed in the detection domain in the range of negative values of $\Delta\alpha_{\text{rf}}$ up to 10° , above which strong PSD signals were measured. Third, no PSD signals within experimental resolution were measured in the detection domain for values of $\Delta\alpha_{\text{rf}} \gtrsim 25^\circ$. How can one interpret these data?

For the negative values of $\Delta\alpha_{\text{rf}}$, the spin supercurrents flow from the source domain towards the detection one. Thus, the spin-precession waves excited in the source domain are dragged by the spin supercurrents, and they travel downstream to the detection domain, where they are detected. The amplitude of the detected waves is reduced by process of the energy dissipation inside the channel due to spin diffusion (for details, see [36]), and by the spin flow modifying the frequency of spin-precession waves which is slightly different from the resonance frequency of the standing waves.

The deep signal minimum in the source domain and corresponding maximum in the detection domain for

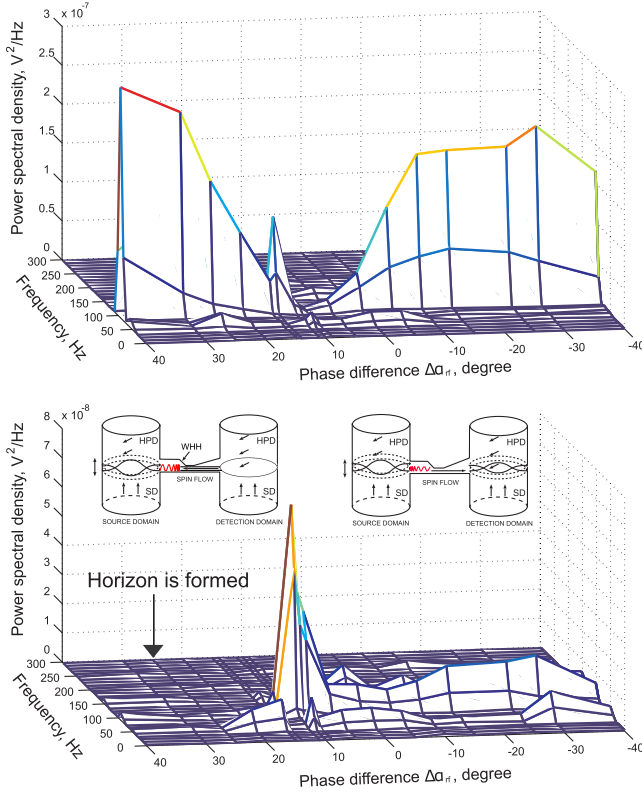


FIG. 3. The power spectral density of the free decay signals as a function of the phase difference measured from the source domain (upper) and the detection domain (bottom). Insets show a schematic illustration of the spin wave dynamics in channel.

$\Delta\alpha_{rf} \sim 10^\circ\text{--}15^\circ$ is the consequence of zero spin flow between domains that leads to a resonance match [42]. Therefore, when the spin-precession waves are excited in the source domain at this condition, all energy is transferred to and absorbed by the detection domain at once. For $\Delta\alpha_{rf} > 10^\circ$ the direction of the spin flow is reversed, i.e., the spin supercurrents flow towards the source domain and the emitted spin-precession waves propagate against this flow. The change in direction of the spin supercurrents is also seen on the phase of the decay signal from the source domain as the gradual phase shift by 180° [36].

As one can see from Fig. 3, there are no PSD signals detected in the detection domain for $\Delta\alpha_{rf} \gtrsim 25^\circ$. We interpret this as a formation of the white hole horizon (WHH) in the channel: spin-precession waves sent from the source domain towards the detection domain are blocked by the spin flow and never reach the detection domain. This interpretation is supported by calculation using the above presented model: the white hole horizon is formed in a place where and when the condition $c^2 = u^2$ is satisfied. For given experimental parameters and assuming that $\nabla\alpha_{rf}$ is localized on the length of $dl = 0.5$ mm, in order to satisfy the condition $c^2 = u^2$ for the phase difference $\Delta\alpha_{rf} \sim 30^\circ$, the estimated length of the precessing layer L is $L \sim 100$ μm , which reasonably corresponds to the experimental value [36].

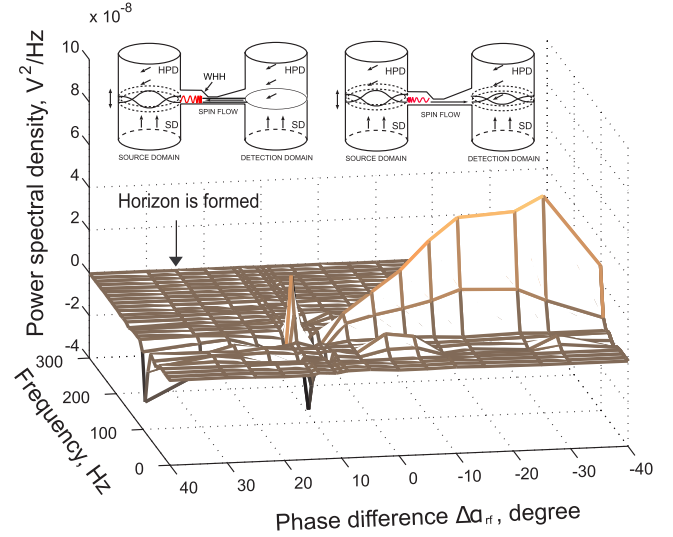


FIG. 4. The cross-correlation power spectral density of the source and detector free decay signals as a function of the phase difference $\Delta\alpha_{rf}$.

Finally, Fig. 4 shows the cross power spectral density between free decay signals measured in source and detector domains as a function of the phase difference $\Delta\alpha_{rf}$. For values of $\Delta\alpha_{rf} < 0^\circ$, i.e., when the spin flow drags excited spin-precession waves from the source domain towards the detection domain, the decay signals from both domains are correlated. For values of $\Delta\alpha_{rf} > 0^\circ$, reduction and following reversion of the spin flow affects the dynamics of the propagation of the spin-precession waves that leads to the change in correlation between the decay signals detected in both domains. When the spin flow approaches zero value, due to the resonance match between the domains, the energy is transferred in both directions, manifested as correlation and anticorrelation peaks. However, when the white horizon is formed ($\Delta\alpha_{rf} > 25^\circ$), the decay signals are anticorrelated. We may interpret this in a way that the rise of the decay signal in the source domain is paid by the spin flow flowing from the detection domain towards the source domain—in agreement with theoretically predicted amplification of the wave on the horizon paid by the energy of the flow [43,44]. This interpretation is supported by dependence presented in Fig. 3 (upper dependence), where a notable feature regarding the absolute values is shown: when spin current flows from the detection domain to the source domain, the waves in the source domain have a tendency to have a higher power spectral density amplitude than those for the spin current flowing in the opposite direction. However, to confirm the physical origin of the observed phenomena, additional measurements have to be done.

In conclusion, we performed the experiment in a limit of absolute zero temperature probing the black- and white-hole horizon analogs in superfluid $^3\text{He-B}$ using the spin-precession waves propagating on the background of the spin supercurrents between two mutually connected

HPDs and provided the evidence of the white hole horizon formation for spin precession waves. Moreover, the presented theoretical model and experimental results demonstrate that the spin-precession waves propagating on the background of the spin supercurrents between two HPDs possess all the physical features needed to elucidate the physics associated with the presence of the event horizons, e.g., to test the spontaneous Hawking process. In fact, assuming that the spin supercurrent velocity of the order of $u \sim 1$ m/s varies on the length of $dl \sim 10^{-4}$ m, one can estimate the temperature of the Hawking radiation in this system to be of the order of 10 nK. It is a temperature only 4 orders of magnitude lower than the background temperature, and this makes the presented system a promising tool for studying this radiation. Here, the spontaneous Hawking radiation can be investigated by means of the cross-correlation statistical measurements of the power spectral density in both HPDs, while simultaneously performing a small, steplike change in the phase of the spin precession in one of the HPDs, thus, generating a perturbation at the horizon.

We acknowledge support provided by the following projects: European Microkelvin Platform (H2020 Project No. 824109), APVV-16-0372, VEGA-0128, and Promatech No. 26220220186. We wish to thank Š. Bicák and G. Pristáš for technical support. Support provided by the U.S. Steel Košice s.r.o. is also gratefully acknowledged.

*skyba@saske.sk

- [1] S. W. Hawking, *Nature (London)* **248**, 30 (1974).
 [2] S. J. Robertson, *J. Phys. B* **45**, 163001 (2012).
 [3] W. G. Unruh, *Phys. Rev. Lett.* **46**, 1351 (1981).
 [4] R. Schützhold and W. G. Unruh, *Phys. Rev. D* **78**, 041504 (R) (2008).
 [5] M. Visser, *Classical Quantum Gravity* **15**, 1767 (1998).
 [6] R. Schützhold and W. G. Unruh, *Phys. Rev. D* **66**, 044019 (2002).
 [7] G. Rousseaux, Ch. Mathis, P. Maïssa, T. Philbin, and U. Leonhardt, *New J. Phys.* **10**, 053015 (2008).
 [8] G. Rousseaux, P. Maïssa, Ch. Mathis, P. Couillet, T. G. Philbin, and U. Leonhardt, *New J. Phys.* **12**, 095018 (2010).
 [9] L. P. Euvé, F. Michel, R. Parentani, T. G. Philbin, and G. Rousseaux, *Phys. Rev. Lett.* **117**, 121301 (2016).
 [10] S. Weinfurter, E. W. Tedford, M. C. J. Penrice, W. G. Unruh, and G. A. Lawrence, *Phys. Rev. Lett.* **106**, 021302 (2011).
 [11] G. E. Volovik, *JETP Lett.* **82**, 624 (2005).
 [12] G. Jannes, R. Piquet, P. Maïssa, C. Mathis, and G. Rousseaux, *Phys. Rev. E* **83**, 056312 (2011).
 [13] M. V. Berry, *New J. Phys.* **20**, 053066 (2018).
 [14] H. S. Nguyen, D. Gerace, I. Carusotto, D. Sanvitto, E. Galopin, A. Lemaître, I. Sagnes, J. Bloch, and A. Amo, *Phys. Rev. Lett.* **114**, 036402 (2015).
 [15] G. E. Volovik, *JETP Lett.* **104**, 645 (2016).
 [16] T. G. Philbin, Ch. Kuklewicz, S. Robertson, S. Hill, F. Konig, and U. Leonhardt, *Science* **319**, 1367 (2008).
 [17] U. Leonhardt and P. Piwnicki, *Phys. Rev. Lett.* **84**, 822 (2000).
 [18] L. J. Garay, J. R. Anglin, J. I. Cirac, and P. Zoller, *Phys. Rev. Lett.* **85**, 4643 (2000).
 [19] S. Giovanazzi, *Phys. Rev. Lett.* **94**, 061302 (2005).
 [20] O. Lahav, A. Itah, A. Blumkin, C. Gordon, S. Rinott, A. Zayats, and J. Steinhauer, *Phys. Rev. Lett.* **105**, 240401 (2010).
 [21] J. Steinhauer, *Nat. Phys.* **12**, 959 (2016).
 [22] A. Roldán-Molina, A. S. Nunez, and R. A. Duine, *Phys. Rev. Lett.* **118**, 061301 (2017).
 [23] P. Skyba, in *Quantum Analogues: From Phase Transitions to Black Holes and Cosmology*, edited by W. G. Unruh and R. Schützhold (Springer, Berlin, Heidelberg, 2007), Vol. 718, pp. 75–92.
 [24] A. S. Borovik-Romanov, Yu. M. Bunkov, V. V. Dmitriev, and Yu. M. Mucharskii, *JETP Lett.* **40**, 1033 (1984).
 [25] I. A. Fomin, *JETP Lett.* **40**, 1037 (1984).
 [26] A. Feher, R. Harakály, L. Lokner, E. Gažo, M. Kupka, J. Nyéki, P. Skyba, Yu. M. Bunkov, and O. D. Timofeevskaya, *J. Low Temp. Phys.* **108**, 461 (1997).
 [27] I. A. Fomin, *JETP Lett.* **45**, 135 (1987).
 [28] Yu. M. Bunkov, V. V. Dmitriev, and Yu. M. Mukharskii, *JETP Lett.* **43**, 168 (1986).
 [29] Yu. M. Bunkov, V. V. Dmitriev, and Yu. M. Mukharskii, *Physica (Amsterdam)* **178B**, 196 (1992).
 [30] V. V. Dmitriev, V. V. Zavjalov, and D. Ye. Zmееv, *J. Low Temp. Phys.* **138**, 765 (2005).
 [31] L. Lokner, A. Feher, R. Harakály, M. Kupka, R. Scheibel, Yu. M. Bunkov, and P. Skyba, *Europhys. Lett.* **40**, 539 (1997).
 [32] E. Gažo, M. Kupka, M. Medeová, and P. Skyba, *Phys. Rev. Lett.* **91**, 055301 (2003).
 [33] M. Človečko, E. Gažo, M. Kupka, and P. Skyba, *Phys. Rev. Lett.* **100**, 155301 (2008).
 [34] M. Kupka and P. Skyba, *Phys. Rev. B* **85**, 184529 (2012).
 [35] A. S. Borovik-Romanov, Yu. M. Bunkov, A. De Waard, V. V. Dmitriev, V. Makróczyová, Yu. M. Mukharskii, and D. A. Sergackov, *JETP Lett.* **47**, 478 (1988).
 [36] See Supplemental Material at <http://link.aps.org/supplemental/10.1103/PhysRevLett.123.161302> for more details and for a brief description of energy dissipation processes in HPD, which includes Refs. [37,38].
 [37] T. Ohmi, M. Tsubota, and T. Tsuneto, *Jpn. J. Appl. Phys.* **26**, Suppl. 26-3, 169 (1987).
 [38] A. Leggett and S. Takagi, *Phys. Rev. Lett.* **34**, 1424 (1975).
 [39] P. Skyba, J. Nyéki, E. Gažo, V. Makróczyová, Yu. M. Bunkov, D. A. Sergackov, and A. Feher, *Cryogenics* **37**, 293 (1997).
 [40] M. Človečko, E. Gažo, M. Kupka, and P. Skyba, *J. Phys. Conf. Ser.* **150**, 032016 (2009).
 [41] P. Skyba, *Rev. Sci. Instrum.* **62**, 2666 (1991).
 [42] The 10° shift from $\Delta\alpha_{\text{rf}} = 0$ for zero spin flow is caused by a small discrepancy in the resonance frequency settings of two resonance circuits used for HPD excitation.
 [43] W. G. Unruh, arXiv:1107.2669.
 [44] J. Steinhauer, *Nat. Phys.* **10**, 864 (2014).